Preparation, Characterization, and Application of Enzyme Nanoparticles

Neelam Yadav*, Jagriti Narang†,1, Anil Kumar Chhillar*, C.S. Pundir‡,1
*Centre for Biotechnology, Maharshi Dayanand University, Rohtak, Haryana, India
†Amity Institute of Nanotechnology, Amity University, Noida, Uttar Pradesh, India
‡Department of Biochemistry, Maharshi Dayanand University, Rohtak, Haryana, India
[1]Corresponding authors: e-mail address: jags_biotech@yahoo.co.in; pundircs@rediffmail.com

Contents

Methods in Enzymology
ISSN 0076-6879
https://doi.org/10.1016/bs.mie.2018.07.001

Abstract

Enzymes are fundamental biocatalysts, which regulate various metabolic reactions. They exhibit high substrate specificity, sensitivity, and exceptional catalytic activity under ideal conditions and, hence, have been used as industrial catalysts. Enzyme nanoparticles have attracted the scientific community as they can be used for environment protection, biochemical engineering, and biomedicine. It is necessary to understand the nature of enzyme nanoparticles interactions with their analyte. Various types of enzyme/protein nanoparticles have been immobilized onto a matrix (electrode or membrane) for the fabrication of biosensors. Among the various nanoparticles and nanomaterials, organic nanoparticles have received more attention due to their fascinating properties. Therefore, the future research should be focused to develop advanced biosensors based on enzyme nanoparticles that could be used for early diagnosis and management of chronic diseases. This chapter explains various enzyme nanoparticles-based biosensors, such as GOX, HRP, uricase, cholesterol oxidase, hemoglobin, and their biomedical applications.

1. INTRODUCTION

1.1 Introduction to Enzyme Kinetics

Enzymes are biological machines, which increase the rate of chemical reactions approximately by as much as 10^8 times by decreasing the activation energy (E_a). E_a is defined as the minimum amount of energy required for a substrate to reach its transition state. Metabolic reactions require small quantities of enzymes. Enzymes (E) bind with a specific substrate (S) to form E–S conjugate which is transformed into product (P); during product formation, enzymes undergo distinct forms of catalysis. The activity of an enzyme depends upon its characteristic parameters such as optimum pH, temperature, incubation time, and appropriate value of the Michaelis–Menten

constant (K_m). K_m is defined as the concentration of substrate required for achieving one-half the maximum velocity (V_{max}). Generally, enzymes show a hyperbolic relationship between their activity and substrate concentration and follow Michaelis–Menten kinetics during the reaction given by Eq. (1):

$$v = \frac{V_{max}[S]}{K_m + [S]} \tag{1}$$

In the above equation v is the initial velocity of the reaction, V_{max} is the maximum velocity, [S] is the substrate concentration, and K_m is the Michaelis–Menten constant. The activity of an enzyme also depends on activators, which increase the rate of the reaction, or inhibitors, which decrease the rate of the reaction. Enzymes often show exceptional substrate selectivity, which means that they bind to specific substrate/analyte but ignore all the others. This is a limitation for most enzymes because each substrate might require a different enzyme to catalyze the corresponding reaction.

1.2 What Are Nanoparticles?

Nanotechnology is a branch of multidisciplinary sciences including life sciences, material science, and information technology. It is implemented at the atomic, molecular, and supramolecular levels on nanoscale, i.e., 1–100 nm. This technology is being used to understand, create, and use material structures, tools, and systems with vital novel properties and applications (Silva, 2004). Hence, it is a promising field of science, which is capable of resolving problems and issues that are difficult to solve in engineering and medical sciences (Nikalje, 2015). Every biological and artificial system indicates association at the nanoscale, such as nanocrystals, nanotubes, or nanobiomotors. Nanoparticles (NPs) are often made by combining molecules into objects, arranged in a functional order by considering various length scales, or dismantle bulk material into particles of nanoscale. The subunits of the particles are held together by means of weak molecular forces including van der Waal forces, hydrogen bonds, electrostatic dipoles, fluidics, and diverse surface forces (Roco, 2003). Various nanostructures such as nanotubes, nanofibers, nanorods, and NPs have been scrutinized to investigate the characteristic features and their applications. The NPs may be organic, inorganic, or a mixed phase; however, organic NPs including protein/enzyme have attracted attention in the past decades for the

fabrication of improved biosensors (Pundir, 2015; Shukla, Deshpande, Shukla, & Tiwari, 2012; Shukla, Mishra, Mamba, & Omotayo, 2014).

1.3 Enzyme Nanoparticles

Covalent linking was used to make enzyme nanoparticles (ENPs) of size <100 nm (Deshapriya et al., 2015; Stromer & Kumar, 2016), but enzyme particles formed by desolvation are often in the range of 100–200 nm (Pundir, 2015). These ENPs exhibit several exceptional characteristic properties such as optical, electronic, electric, thermal, chemical, mechanical, and catalytic while supporting a large surface area, compared to the bulk material but less than those of the free enzymes. These properties of ENPs improve the activity of enzyme-based biosensors. Direct immobilization of proteins or enzymes onto NPs may cause denaturation which could result in enzyme inactivation. This problem has been resolved by preparing ENPs and self-cross-linked before their attachment. ENPs-based biosensors have enhanced the analytical parameters such as detection limit and current response (Sharma, Shrivastav, Gupta, & Srivastava, 2011). NPs of horseradish peroxidase (HRP) were synthesized very first time (Liu, Lin, Ostatna, & Wang, 2005). Subsequently, NPs of glucose oxidase (GOD) (Sharma et al., 2011), cholesterol oxidase (ChOx) (Chawla, Rawal, Sonia, & Pundir, 2013), uricase (Chauhan, Kumar, & Pundir, 2014), and hemoglobin (Hb) (Yadav, Chhillar, & Pundir, 2018)-based amperometric biosensors have been developed.

These ENPs differ from single enzyme nanoparticles (SENs), which are single enzyme encapsulated with nanoscale organic/inorganic macromolecules that improve the catalytic activity and thermal stability. Trypsin SENs were used to improve the enzyme stability at increased temperature, while chymotrypsin SENs have been used to improve cellulose degradation (Blanchette, Lacayo, Fischer, Hawang, & Thelen, 2012; Khosravi, Vossoughi, Sharokhian, & Alemzadeh, 2012; Kim & Grate, 2003).

2. EXPERIMENTAL

2.1 Chemicals and Reagents

(i) Enzyme (1–2 mg)
(ii) Ethanol, desolvating agent (4 mL)
(iii) 2.5% glutaraldehyde (1.8 mL)
(iv) Cysteine or cysteamine dihydrochloride (0.12 g)
(v) Analyte to detect

2.2 Equipment

(i) Support material [electrode (Au, pencil graphite, screen printed, etc.), fluorine tin oxide nitrocellulose (NC) membrane]
(ii) Weighing balance
(iii) Magnetic stirrer
(iv) Magnetic beads
(v) Centrifuge
(vi) Potentiostat
(vii) Water bath
(viii) Ultraviolet (UV)-spectrophotometer

2.3 Methods to Prepare ENPs

NPs of soluble proteins have been prepared by their aggregation by following methods:

(i) Emulsification in plant oil (Scheffel, Rhodes, Natrajan, & Wagner, 1972)
(ii) Desolvation by ethanol or natural salts and the aggregated protein is cross-linked by glutaraldehyde (Coester, Langer, & Von, 2000)
(iii) Coacervation via anhydrous ethanol, glutaraldehyde, and ethanolamine (Sailaja, Amareshwar, & Chakravarty, 2011)
(iv) Cross-linking in water and oil emulsion at high pressure (Ezpeleta et al., 1999)

ENPs were prepared by desolvation by using ethanol as desolvating agent followed by cross-linking with glutaraldehyde (Liu et al., 2005).

2.4 Preparation of ENPs by Desolvation

Various steps of desolvation method for ENP preparation are described below.

2.4.1 Desolvation

The lyophilized form of an enzyme (1–2 mg mL^{-1}) was dissolved in reaction buffer. Ethanol was added as a desolvating agent, dropwise at a rate of 0.1–0.5 mL min^{-1} in 1:2 ratio, under constant stirring at a speed of 500 rpm at 4°C. Addition of the desolvating agent facilitated the formation of enzyme/protein aggregates to form NPs in the range of 1–100 nm.

2.4.2 Cross-linking

After the formation of enzyme aggregates they are cross-linked by the addition of 2.5%–8.0% glutaraldehyde (1.8 mL) under constant stirring at 500 rpm at 4°C in an ice bath for 24 h. Addition of glutaraldehyde resulted in intermolecular cross-linking within ENPs by forming Schiff base linkages.

2.4.3 Functionalization

The ENPs were further functionalized by adding 0.12 g cysteamine dihydrochloride or cysteine under constant stirring, which introduced $-NH_2$ or –SH groups on the ENPs. These functions enhance the attachment of the ENPs on the surface of the electrode.

2.4.4 Purification

The cross-linked, surface functionalized ENPs were separated by centrifuging the above preparation at 14,000 rpm at 4°C for 10 min. The supernatant was removed and the pellet dispersed into the buffer by ultrasonication for 5 min. Finally, the ENPs were separated by centrifugation at 12,000 rpm, 15,000 × *g* at 4°C for 10 min. Schematic representation of the formation of ChOx NPs was shown in Fig. 1.

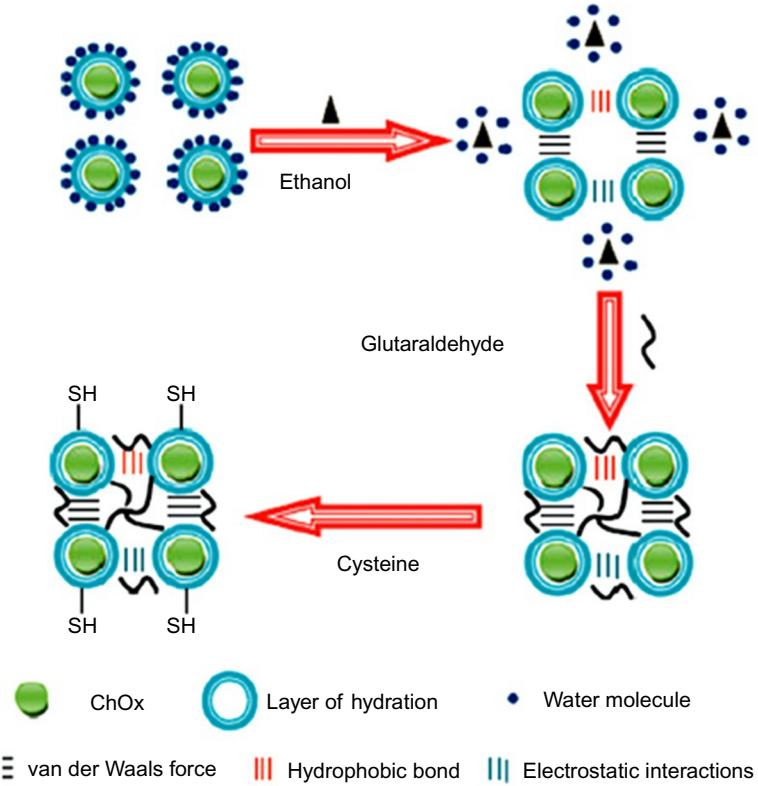

Fig. 1 Schematic representation of formation of cholesterol oxidase nanoparticles (CHOxNPs) by the desolvation method and introduction of –SH group by cysteine on the surface of ChOxNPs (Chawla et al., 2013).

2.5 Characterization of ENPs

ENPs have characteristic features, which were determined by various techniques as described below.

2.5.1 Transmission Electron Microscopy

The shape and size of ENPs were characterized by transmission electron microscopy (TEM) images. The spherical shape and the diameter of ENPs aggregates range from 100 to 200 nm (Fig. 2). The diameter of free enzyme molecules is in the range of 2–18 nm. A comparison of TEM size of free enzymes and ENPs is shown in Table 1.

2.5.2 Colorimetric Methods

ENPs exhibited characteristic colors. For instance, ENPs of HRP were white in color. The ENP aggregates acquired the color due to a combination of light scattering and absorption. The particles are too large, on the order of the wavelengths of visible light.

2.5.3 UV Absorption Spectra

Different enzymes and their ENPs showed absorbance at their characteristic wavelengths. For instance, native Hb exhibited a Soret absorbance peak

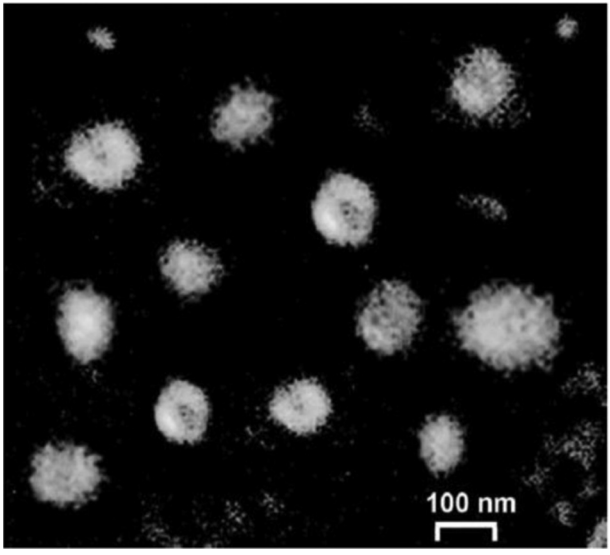

Fig. 2 Transmission electron microscopic (TEM) images illustrating configuration, size, and color of horseradish peroxidase nanoparticles (Liu et al., 2005).

Table 1 A Comparison of Average Diameter of Enzyme Nanoparticles (ENPs) and Free Enzyme by TEM

ENPs	Diameter of ENPs (nm)	Diameter of Free Enzyme	Ref.
Horseradish peroxidase	100	14.2	Liu et al. (2005)
Glucose oxidase	117	2–8	Kundu, Yadav, and Pundir (2012)
Cholesterol oxidase	100–200	–	Chawla et al. (2013)
Uricase	100	14–18	Chauhan et al. (2014)
Hb	97	—	Yadav et al. (2018)
ChE	35–40	—	Aggarwal, Malik, Prashant, Jaiwal, and Pundir (2016)
ChOx	56.97		Aggarwal et al. (2016)
Lipase	83–218	—	Pundir and Aggarwal (2017)
GK	144–329	—	Pundir and Aggarwal (2017)
GPO	22–68	—	Pundir and Aggarwal (2017)

at 410 nm, while hemoglobin nanoparticles (HbNPs) showed no Soret band but had an absorbance peak at 280 nm which is due to the protein absorption. The loss of Soret band could be due to the large size of HbNPs (Yadav et al., 2018). Fig. 3 shows the comparative UV spectra of native Hb and HbNPs.

2.5.4 FTIR Spectra

The FTIR spectra of native Hb and HbNPs are compared. The native Hb showed the characteristic peaks at 1062, 1317, 1553, 1679, and 3497 cm^{-1}, while HbNPs had peaks at 1090, 1305, 1561, 1701, and 3488 cm^{-1}. These characteristic peaks showed the presence of various functional groups of native Hb and HbNPs. The band at 1062 cm^{-1} indicates the presence of amine groups. In addition, there was a band located at 3497 cm^{-1}, which could be assigned to the O–H stretching, indicating the presence of hydroxyl groups. The FTIR spectra of the Hb and HbNPs exhibited a key shift at carbonyl, hydroxyl, and amino groups of the protein, which may be due to ethanol, glutaraldehyde, and cysteamine dihydrochloride treatment during the synthesis of HbNPs (Fig. 4).

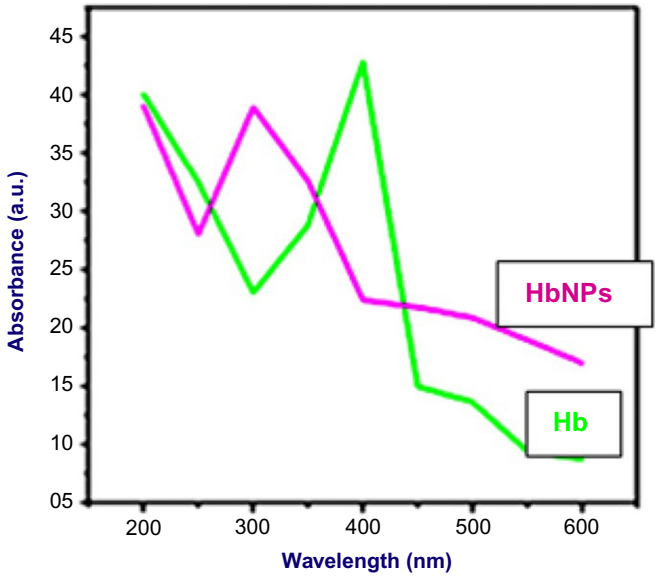

Fig. 3 UV spectra of native Hb and HbNPs (Yadav et al., 2018).

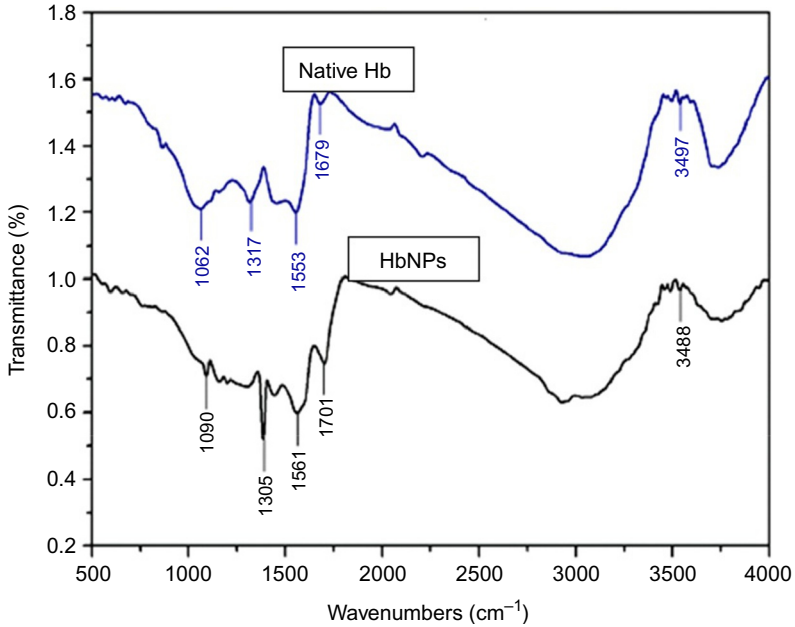

Fig. 4 FTIR spectra of monomeric native Hb and HbNPs (Yadav et al., 2018).

3. IMMOBILIZATION OF ENPs

The attachment of ENPs on to an inorganic/organic matrix is to be done in such a way that the attached ENPs do not lose their function and the resulting biocatalyst is usable multiple times. ENPs are immobilized onto support matrix via adsorption, entrapment, microencapsulation, covalent binding, and metal binding and aggregated by bifunctional reagents. For instance, aggregates of NPs of HRP (Liu et al., 2005), Hb (Yadav et al., 2018), lactate oxidase (Dagar & Pundir, 2017), cholesterol oxidase (ChOx) (Aggarwal et al., 2016), uricase (Chauhan et al., 2014), and many more have been immobilized covalently onto Au electrode. Besides, NPs of GOD isolated from *Aspergillus niger* have been immobilized on Pt electrode and NC membranes.

3.1 Characterization of ENPs Immobilized Onto Matrix

Confinement of ENPs onto their support material was confirmed by scanning electron microscopy (SEM). SEM images of bare electrode or membrane showed the uniform surfaces, whereas electrodes immobilized with ENPs showed globular, beaded configurations and clusters of aggregated ENPs on the entire surface (Fig. 5). This confirms the immobilization of ENP onto support material (electrode/membrane) (Yadav et al., 2018).

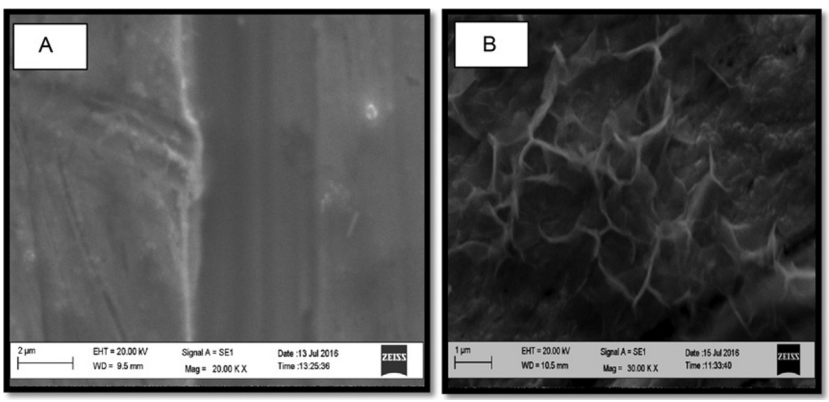

Fig. 5 (A) SEM images of bare Au electrode and (B) HbNPs immobilized Au electrode. *From Yadav et al. (2018).*

3.2 Kinetic Properties of ENPs

For immobilized ENPs, one needs to determine optimum pH, temperature, the working range, reusability, storage stability, K_m, and response time. The kinetic parameters were studied after covalent immobilization either onto metal wire like Au/Pt or on NC membranes. A comparison of various parameters is given in Table 2.

Table 2 K_m Value of Enzyme Nanoparticles (ENPs)-Based Biosensors

ENPs-Based Biosensor	K_m Value (m*M*)	Ref.
HbNPs/AuE	0.1 ± 0.001	Narwal, Yadav, Thakur, and Pundir (2017)
Uricase NPs/AuE	0.058	Chauhan et al. (2014)

3.2.1 Optimum pH

ENPs showed maximum activity at a particular pH, and ENPs attached to supports exhibited some change in their optimum pH in comparison to a monomeric enzyme. For instance, elevated pH with a difference of 0.4 for HRP (Liu et al., 2005), pH with a difference of 0.5 for GOD (Kundu et al., 2012), ChOx (Chawla et al., 2013), uricase (Chauhan et al., 2014), and HbNPs (Fig. 6) (Yadav et al., 2018). This alteration in optimum pH was because of the modified configuration of ENPs after their immobilization.

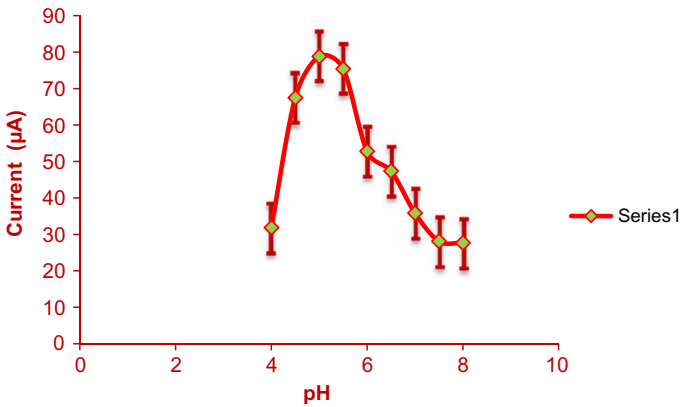

Fig. 6 Effect of pH on current response of HbNPs/AuE in 0.1 *M* sodium acetate buffer. *From Yadav et al. (2018).*

3.2.2 Optimum Temperature and Thermostability

At the optimum temperature, the attached ENPs showed significant activity improvements when compared to the free enzyme. The optimum temperature for ChENPs + ChOxNPs/AuE was 40°C (Aggarwal et al., 2016), and for lipase NPs + GKNPs + GPONPs/AuE, it was 35°C (Pundir & Aggarwal, 2017). ENPs exhibited higher stability in their immobilized form as compared to the free enzyme. For example, the thermostability of GOD NPs was greater as compared to free GOD because of inter- and intramolecular covalent bonding that inhibited the structural alterations of the enzyme at elevated temperatures (Fig. 7).

3.2.3 Response Time

ENP immobilization had shorter response times. For example, response time of HbNPs/AuE was 2 s (Yadav et al., 2018), while response time of Hb/cMWCNT-Fe_3O_4NP/CHIT/Au electrode was 8 s (Batra, Lata, Sharma, & Pundir, 2012), ChENPs + ChOxNPs/AuE was 5 s (Aggarwal et al., 2016), lipase NPs/GKNPs/GPONPs/AuE was 5 s (Pundir & Aggarwal, 2017), while lipase-based biosensor showed response time 30 min (Chen et al., 2014), uricase NPs/AuE was 7 s (Chauhan et al., 2014), whereas response time of

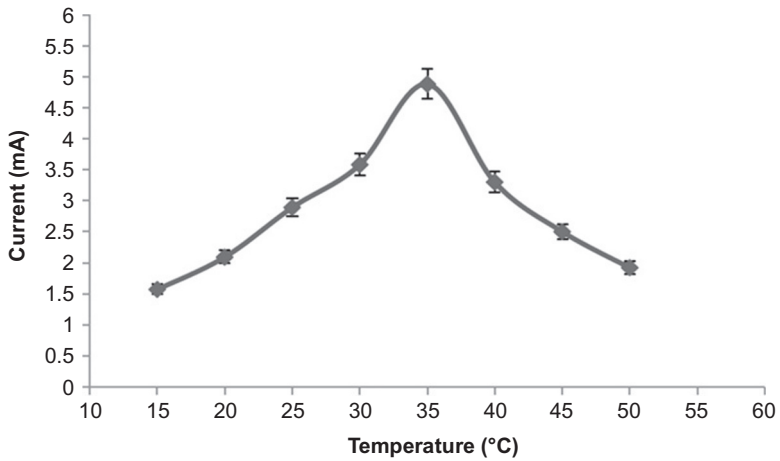

Fig. 7 Effect of temperature on current response of lipase NPs, GKNPs, and GPONPs/AuE. *From Pundir, C. S., & Aggarwal, V. (2017). Amperometric triglyceride bionanosensor based on nanoparticles of lipase, glycerol kinase, glycerol-3-phosphate oxidase.* Analytical Biochemistry, 517, *56–63.*

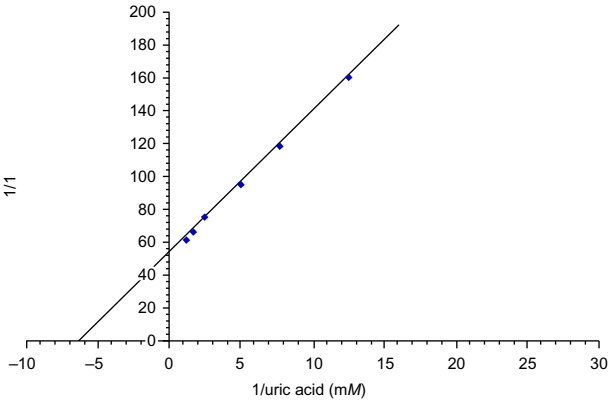

Fig. 8 Lineweaver–Burk plot of the effect of uric acid concentration on response of uric acid biosensor based on uricase NPs-modified Au electrode. K_m was calculated using the following equation: $1/v = K_m/V_{max}.1/[S] + 1/V_{max}$, where v is the biosensor response in current (mA), and S is the uric acid concentration in m*M*. Slope of LB plot $= K_m/V_{max}$; intercept of the plot $= 1/V_{max}$. *From Chauhan, N., Kumar, A., & Pundir, C. S. (2014). Construction of an uricase nanoparticles modified Au electrode for amperometric determination of uric acid.* Applied Biochemistry and Biotechnology, 174, *1683–1694.*

uricase biosensor was 330 s (Cete, Yaşar, & Arslan, 2006) and ChOxNPs/AuE was 8 s (Chawla et al., 2013), while monomeric ChOx-based biosensor exhibited response time of 30 s (Guo, Chen, Li, Nie, & Yao, 2004).

3.2.4 K_m Values

Immobilization also decreased or retained the K_m values of ENPs as compared to those of the corresponding free enzymes. The K_m values of uricase NPs immobilized onto Au electrode were calculated from the Lineweaver–Burk plot (Fig. 8), which was similar to that of the free enzyme (Chauhan et al., 2014).

3.2.5 Working Range

Working range is the concentration range over which the sensor is responsive. Limit of detection (LOD) is the lowest concentration detected by the biosensor calculated by using the formula: $LOD = 3.3 \times SD/S$, where SD is the standard deviation of the response, and S is the slope of the calibration curve (Valipour, 2015). The working range of immobilized ENPs is narrow as compared to that of the free enzyme. The working ranges of various biosensors are collected in Table 3.

Table 3 Working Range of Various Enzyme Nanoparticles (ENPs)-Based Biosensors

ENPs-Based Biosensor	Working Range	Ref.
HbNPs/AuE	0.1–100 n*M*	Yadav et al. (2018)
HbNPs/AuE	1.0–1200 μ*M*	Narwal et al. (2017)
ChENPs + ChOxNPs/AuE	10–700 mg/dL	Aggarwal et al. (2016)
Lipase NPs + GKNPs + GPO/AuE	10–100 mg/dL	Pundir and Aggarwal (2017)
ChOx NPs/AuE	12.5–700 mg/dL	Chawla et al. (2013)
Uricase NPs/AuE	0.005–0.8 m*M*	Chauhan et al. (2014)

4. STABILITY AND REUSABILITY

4.1 Storage Stability

At lower temperatures, immobilized ENPs showed better storage stability than the free enzyme and these data are collected in Table 4. This is usually the case for most immobilized enzymes.

4.2 Reusability

ENPs immobilized on different matrices avoid the frequent recharging with ENPs, which, in turn, reduces the cost and labor. The reusability of immobilized ENPs was better than free enzymes. Immobilized ENPs can be reused 100–200 times, and hence, ENPs were economic and have been employed in diverse applications.

4.3 Correlation of Measurements With a Standard Method

The performance of the biosensor was correlated by a colorimetric method. The concentration determined by the biosensor was validated by plotting the concentration obtained by the colorimetric method on the x-axis and the concentration obtained by biosensing method on the y-axis (Narwal et al., 2017). The values obtained were analyzed by regression and the correlation coefficient has been calculated by Eq. (2):

$$\text{The correlation coefficient}\,(r) = \frac{n\left(\sum xy\right) - \left(\sum x\right)\left(\sum y\right)}{\sqrt{\left[n\sum x^2 - \left(\sum x\right)^2\right]\left[n\sum y^2 - \left(\sum y\right)^2\right]}} \tag{2}$$

where

x values obtained by HPLC

y values obtained by biosensing

Table 4 Comparison of Kinetic Properties of Immobilized Enzyme Nanoparticles With Those of Free Enzymes

	Glucose Oxidase From *A. niger*		Cholesterol Oxidase from Microorganism		Uricase From *Candida* sp.		Hemoglobin	
Property	**Free**	**Immobilized NPs**	**Free**	**Immobilized NPs**	**Free**	**Immobilized NPs**	**Free**	**Immobilized NPs**
Support used	—	NC membrane	—	Au wire	—	Au wire	Au wire	Au wire
Method of immobilization	—	Covalent	—	Covalent	—	Covalent	Covalent	Covalent
Type of electrode	—	DO metric	—	Amperometric	—	Amperometric	Amperometric	Amperometric
Optimum pH	5.5	6.0	5.5	6.0	8.0	8.5	5.0	
Optimum temperature	3.5	35–45	37	35	30	40	30	20
Incubation time (s)	120	60	300	8	300	7	8	2
K_m (m*M*)	6.2	4.17	—	ND	0.056	0.058	—	—
Linearity (m*M*)	Up to 13.8	0.056–1.39	Up to 6.4	0.69–38.88	Up to 1.5	0.005–0.8	3–90 n*M*	0.1 n*M*–100 m*M*
Limit of detection (m*M*)	0.138	0.55	0.01	0.04	160	0.005	0.02 n*M*	0.1 n*M*
Half-life at 4°C in days	180	180	60	90	60	210	60	120
No. of reuses	—	150	—	180	—	200	—	
Ref.	Kalia, Goyal, and Pundir (1999)	Kundu et al. (2012)	Varma and Nene (2003)	Chawla et al. (2013)	Freitas, Spencer, Vasao, and Abrahao-Neto (2009)	Chauhan et al. (2014)	Batra et al. (2012)	Yadav et al. (2018)

ND, not detected.

5. APPLICATIONS OF ENPs

Biosensors are the quantitative analytical devices, which consist of a biological recognition entity such as enzyme, antibody, phage, aptamer, or single-stranded DNA coupled with appropriate physicochemical, optical, thermometric, piezoelectric, and magnetic transducers (Elif & Mustafa, 2015). In other words, biosensors are chemical sensors in which the biological recognition element uses a biochemical mechanism interfacing the optoelectronic system (Cammann, 1977; Turner, Karube, & Wilson, 1987) (Fig. 9).

There are of various types of biosensors. Among them electrochemical biosensors have been used widely for the analysis of processed foods and have given more attention in various fields, due to their small size, cost-effectiveness, fast response time, possibility of achieving low detection limits, and good functioning (Wang et al., 2014). Various ENP-based biosensors are described below.

5.1 Biosensor Based on Immobilization of Nanoparticles of Cholesterol Esterase and Cholesterol Oxidase

An amperometric biosensor based on covalent immobilization of cholesterol esterase nanoparticles (ChENPs) and cholesterol oxidase (ChOxNPs) onto Au electrode for the determination of cholesterol in serum (Fig. 10) (Aggarwal et al., 2016). The biosensor showed an optimum response within 5 s at pH 5.5, 40°C at 0.25 V vs Ag/AgCl. The linear range of the biosensor was 10–700 mg dL^{-1}. This biosensor was evaluated in terms of various analytical parameters such as analytical recovery of added cholesterol concentration at 100 and 200 mg dL^{-1} were 95% and 96%, with coefficients of variation as <2% and <3%, respectively. The storage stability of working electrode was 60 days at 4°C.

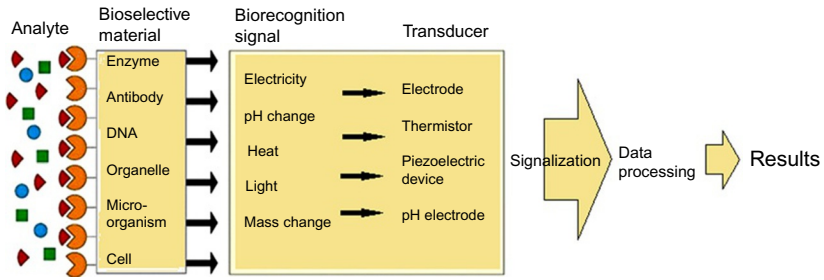

Fig. 9 Principle and working of a biosensor (https://doi.org/10.5772/54127).

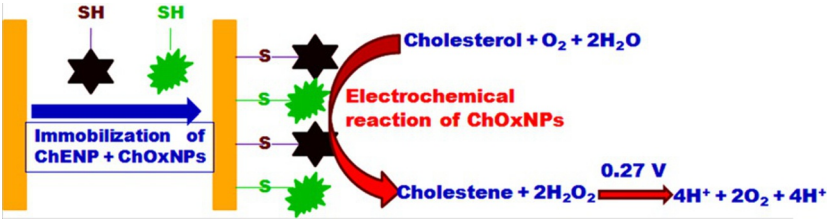

Fig. 10 Schematic representation of immobilization and working of ChENPs- and ChOxNPs-based cholesterol biosensor. *From Aggarwal, V., Malik, J., Prashant, A., Jaiwal, P. K., & Pundir, C. S. (2016). Amperometric determination of serum total cholesterol with nanoparticles of cholesterol esterase and cholesterol oxidase.* Analytical Biochemistry, 500, *6–11.*

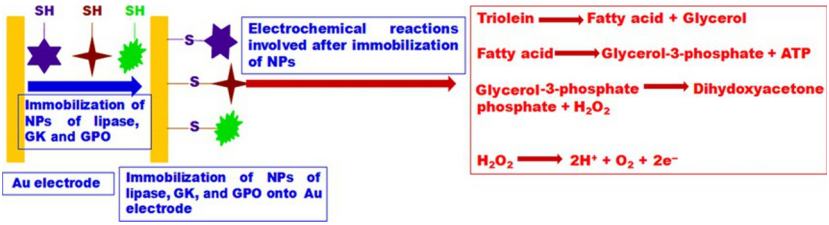

Fig. 11 Schematic representation of attachment of functionalized lipase, glycerol kinase (GK), and glycerol-3-phosphate oxidase (GPO) NPs and their electrochemical reaction onto Au electrode (Pundir & Aggarwal, 2017).

5.2 Biosensor Based on Immobilization of Nanoparticles of Lipase, Glycerol Kinase, and Glycerol-3-Phosphate Oxidase

The porcine pancreas lipase, glycerol kinase (GK) from *Cellulomonas* sp., and glycerol-3-phosphate oxidase (GPO) from *Aerococcus viridans* were prepared by the above desolvation method (Pundir & Aggarwal, 2017) (Fig. 11). These NPs were characterized by TEM and FTIR and immobilized onto Au electrode. The performance of the biosensor was maximum at pH 6.5 at 35°C. The working potential of biosensor was 1.2 V and response time 5 s. Biosensor was evaluated in terms of linear concentration range of 1.0–100 and 100–500 mg dL^{-1}, respectively. The detection limit was 1.0 μg mL^{-1}, and the analytical recovery of added concentration was 95% and 96% at 50 and 100 mg dL^{-1}, respectively. The coefficients of variation were 2% and 2%, respectively. The storage stability of working electrode was 90 days.

5.3 Biosensor Based on Immobilization of Nanoparticles of Hb

An amperometric biosensor was constructed by immobilizing Hb ENPs onto the Au electrode (Narwal et al., 2017) (Fig. 12). The working electrode

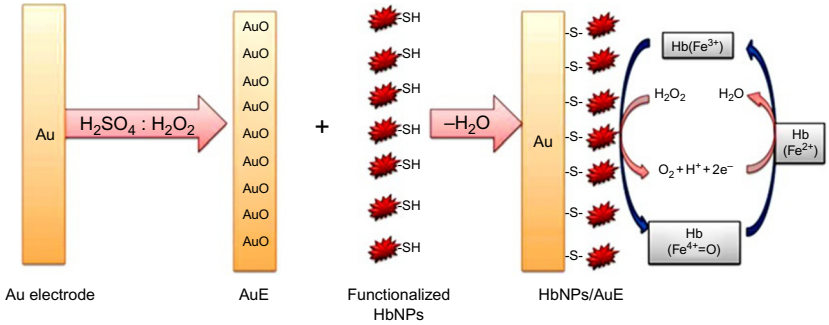

Fig. 12 Schematic representation and electrochemical reaction involved in the fabrication of HbNPs onto Au electrode for the detection of H_2O_2 in the serum sample. *From Narwal, V., Yadav, N., Thakur, M., & Pundir, C. S. (2017). An amperometric H_2O_2 biosensor based on hemoglobin nanoparticles immobilized onto a gold electrode.* Bioscience Reports, 37, *1–10.*

was characterized by cyclic voltammetry (CV), SEM, FTIR spectroscopy, and electrochemical impedance spectroscopy (EIS). The NPs of copper were characterized by TEM and UV-spectroscopy. HbNPs/AuE gave good response within 2.5 s, at pH 6.5 and temperature 30°C when operated at 20 mV s^{-1}. The biosensor was evaluated in terms of its detection limit 1.0 μ*M*, linear range was 1–1200 μ*M*, and the analytical recovery of biosensor was 99% and 98%. The coefficients of variation were 3% and 4%, respectively. The storage stability of working electrode was 90 days.

5.4 Biosensor Based on Immobilized HbNPs for the Determination of Acrylamide in Processed Foods

HbNPs were prepared by the desolvation method and characterized by TEM, UV–visible spectroscopy, FTIR, XRD, and AFM (Yadav et al., 2018). These HbNPs were immobilized covalently onto Au electrode (Fig. 13). The Au electrode was characterized by SEM and EIS. HbNPs/AuE was optimized in terms of its pH 5.0, and working potential 0.26 V at 20°C. The analytical recovery of biosensor was 99% and 98% at 5 and 10 m*M* acrylamide, respectively. The coefficients of variation were 4% and 5%, respectively. The proposed biosensor was used for the detection of acrylamide in processed foods.

5.5 Biosensor Based on Immobilized HRP Nanoparticles

Liu et al. (2005) have constructed an improved amperometric biosensor by immobilizing the HRPNPs covalently onto Au electrode (Fig. 14). The

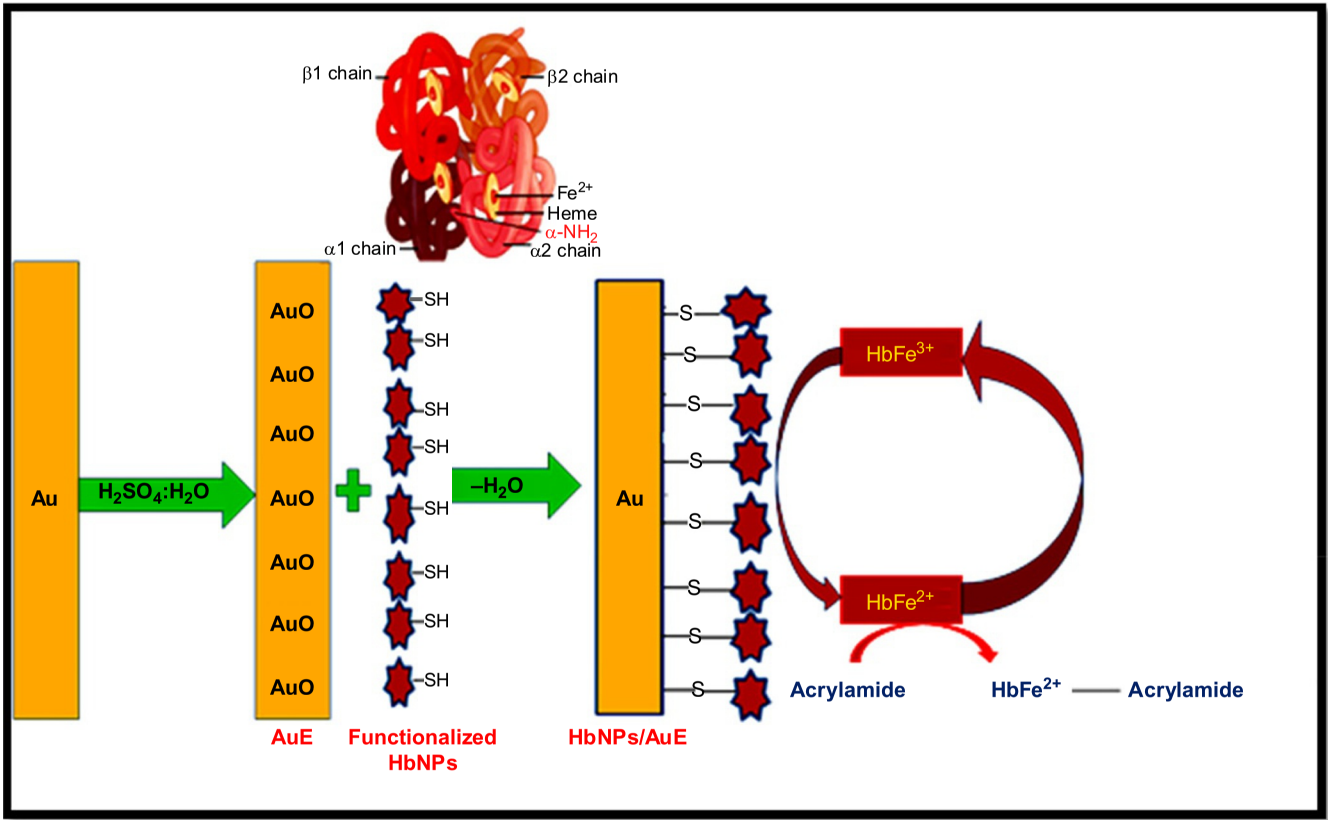

Fig. 13 Schematic representation and electrochemical reaction involved in the fabrication of HbNPs onto Au electrode. *From Yadav, N., Chhillar, A.K., & Pundir, C.S. (2018). Preparation, characterization and application of haemoglobin nanoparticles for detection of acrylamide in processed foods. International Journal of Biological Macromolecules, 107, 1000–1013.*

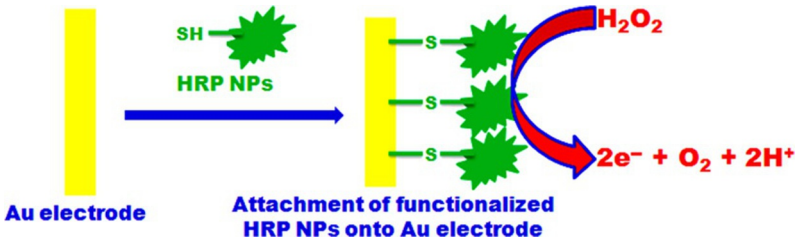

Fig. 14 Schematic representation of attachment of functionalized horseradish peroxidase (HRP) nanoparticles onto Au electrode (Liu et al., 2005).

performance of the biosensor was optimum at pH 7.4 when operated at 0.16 V. The linear range of HRPNPs/AuE was 1–9 μ*M*, detection limit was 0.1 μ*M*, and coefficient of variation was 3%.

5.6 Biosensor Based on Immobilized GOD Nanoparticles

The biosensor was fabricated by using GOD NPs (Kundu et al., 2012; Sharma et al., 2011) (Fig. 15). The biosensor was used for the electrochemical quantification of H_2O_2 produced from glucose. GOD NPs/AuE worked optimally at pH 7.4, and 27°C, with a linear range of 1–35 mg dL^{-1}. The working range of the biosensor was 35 mg dL^{-1}. The LOD of GOD NPs/AuE was 18 μ*M*.

5.7 Biosensor Based on Immobilized ChOx Nanoparticles

An improved amperometric biosensor was fabricated by immobilizing ChOx NPs onto Au electrode (Fig. 16) (Chawla et al., 2013). The ChOxNPs/AuE worked best at pH 6.0, and 35°C, when operated at 0.27 V vs Ag/AgCl. The working range of ChOxNPs/AuE was 12.5–700 mg dL^{-1}, with a detection limit of 1.56 mg dL^{-1}. The storage stability of biosensor was 90 days at 4°C.

5.8 Biosensor Based on Immobilized Uricase Nanoparticles

Chauhan et al. (2014) constructed a highly sensitive biosensor for the determination of uric acid in blood or urine (Fig. 17). The optimum performance of the biosensor was observed within 7 s, at pH 8.5, and 40°C at a potential of 0.2 V. The uricase NPs/AuE had a linear range of 0.005–0.8 m*M*, analytical recovery 100% and 99% at 10 and 29 mg L^{-1} uric acid, high sensitivity 0.003 mA μM^{-1} cm^{-2}, and stored for 210 days at 4°C. The precision of biosensor was 5.6% and 4.7%, respectively.

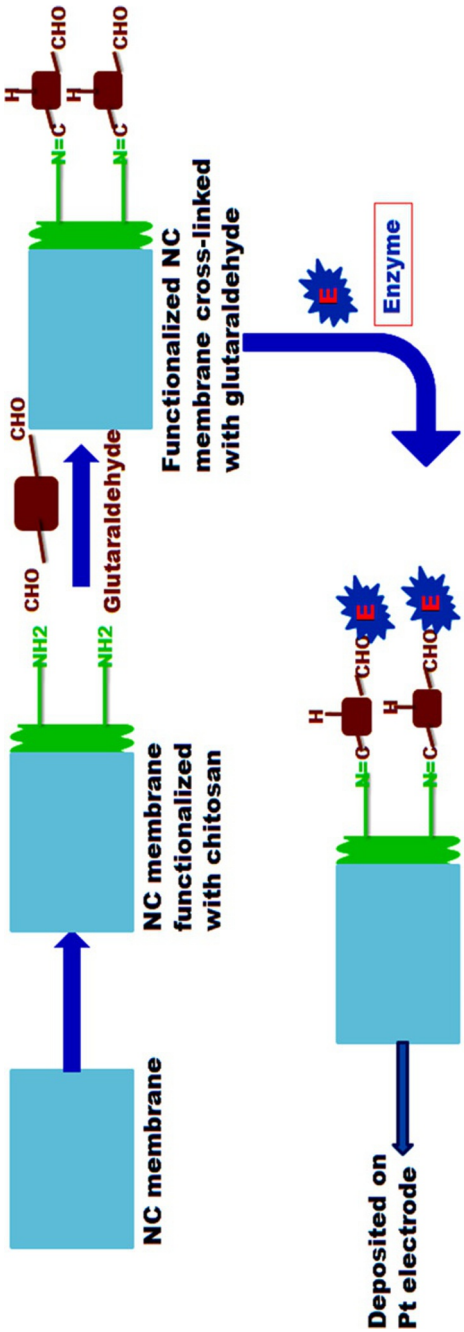

Fig. 15 Schematic representation of attachment of functionalized nitrocellulose (NC) membrane functionalized with chitosan and glutaraldehyde followed by immobilization of glucose oxidase (GOD) NPs and deposited onto Pt electrode (Sharma et al., 2011).

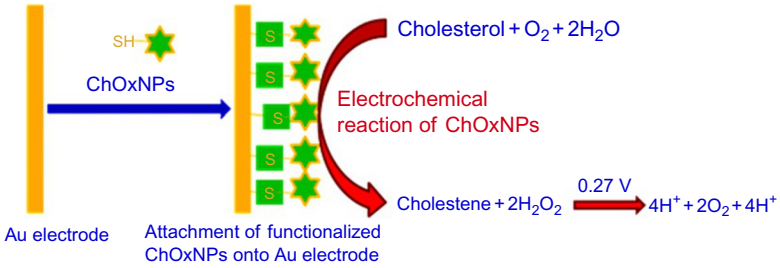

Fig. 16 Schematic representation of attachment of functionalized ChOxNPs and their electrochemical reaction onto Au electrode (Chawla et al., 2013).

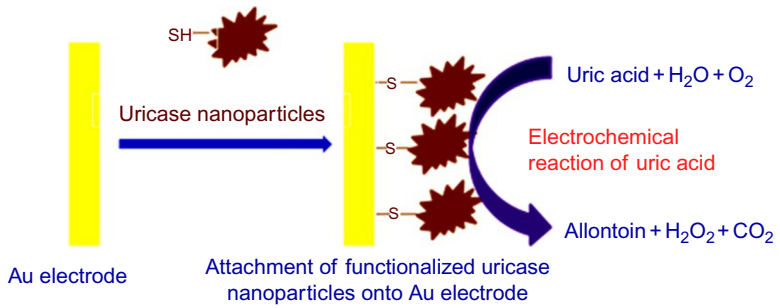

Fig. 17 Schematic representation of attachment of functionalized uricase nanoparticles and electrochemical reaction onto Au electrode (Chauhan et al., 2014).

6. DETAILED PROCEDURE FOR THE DEVELOPMENT OF HbNPs-BASED BIOSENSORS

Acrylamide is carcinogenic, neurotoxic, and reproductive toxicant, and hence, its detection is important. An improved amperometric acrylamide biosensor based on HbNPs is described here (Yadav et al., 2018).

6.1 Reagents

Human Hb from Sigma-Aldrich; acrylamide, potassium hexacyanoferrate(II) trihydrate (Carrez I), acetic acid, zinc sulfate heptahydrate (Carrez II), and glutaraldehyde from Merck; cysteamine dihydrochloride, potassium ferrocyanide, potassium ferricyanide, and copper sulfate from Sisco Research Labs (Mumbai, India); and ethanol from Changshu Yangyuan Chemical (China) have been used. All other chemicals were of analytical reagent grade. Au wire purchased from local jeweler, different brands of biscuits, kurkure, crisps, fried cereals, and diverse bread items were purchased from a local market.

6.2 Instruments Used

A potentiostat/galvanostat (Autolab, AUT83785, Eco Chemie) with a three-electrode system consisting of a Au wire as a working electrode, Pt wire as a counter electrode, and Ag/AgCl as a reference electrode was used. Zeiss EV040 SEM, UV-spectrophotometer (Dynamica HALO DB-20, UK), TEM, and FTIR spectrophotometer (Thermo Scientific, USA) were used. Refrigerated centrifuge (Sigma 3-30K, Germany), Spectronic-20, electronic balance, and temperature-controlled water bath (NSW) were used.

6.3 Preparation and Testing of HbNP Biosensor

Prepare a solution of Hb by dissolving Hb powder (4 mg) in sodium phosphate buffer (2 mL; 0.02 *M*, pH 5.0). Add ethanol (4 mL) dropwise into Hb solution under constant stirring, followed by addition of glutaraldehyde (1.8 mL of 2.5%), and stir for a whole. Add glutaraldehyde (1.8 mL; 2.5%) into this preparation, followed by the addition of cysteamine dihydrochloride (0.12 g), and let it stir for 5–6 h. Then centrifuge the sample (4°C) at 1200 rpm for 10 min and separate the supernatant from the pellet. Dissolve the pellet 0.1 *M* sodium phosphate buffer (pH 7.0) and store at 4°C until it is used. Characterize the samples by UV and FTIR as described in Figs. 3 and 4.

Immobilize the HbNPs onto Au electrode and wash the Au wire with piranha solution (concentrated H_2SO_4 and H_2O_2, in 3:1 ratio), followed by polishing with silica gel. Sonicate the Au wire and wash with distilled water. Dip the Au wire into a suspension of HbNPs, and remove and rinse with 0.1 *M* sodium phosphate buffer (pH 7.0). Characterize the working electrode by SEM (Fig. 5).

Construct the acrylamide biosensor using HbNPs/Au as a working electrode, Ag/AgCl as a reference electrode, and Pt wire as a counter electrode connected to a potentiostat. Measure the current (in mA) as a function of time (in seconds) (Fig. 14). Record the CV of the working electrode in potentiostat galvanostat in the potential range of −0.750 to 0.500 V in 25 mL of 0.2 *M* sodium acetate buffer (pH 6.0) containing 0.1 mL, 3.5 μ*M* acrylamide at a scan rate of 20 mV s^{-1}. Record the response of the biosensor (in current) for acrylamide in the range of 0.1–100 n*M*.

Test the biosensor to measure acrylamide in real samples with various concentrations of processed foods. Crush the samples to form a fine powder and dissolve a known amount of food powder in 100 mL distilled water, placed at room temperature for 20 min to swell to form a suspension.

After, 1 h of stirring at 60°C, centrifuge the suspension at 4500 rpm, at 4°C for 20 min. Remove the supernatant and test for acrylamide concentration, under standard conditions of 25 mL sodium acetate buffer, pH 5.0 at 20°C and by applying a potential of 0.26 V. Add the sample (100 μL) to 25 mL sodium acetate buffer (pH 5.0) and measure the current at 0.26 V at a scan rate of 20 $mV\,s^{-1}$ vs Ag/AgCl. Determine the acrylamide content in the sample from a standard curve. Evaluate the biosensor by investigating its various parameters such as linearity (0.05–100 n*M*), LOD (0.1 n*M*)%, analytical recovery (99% and 98%), and precision (3.85% and 4.67%), and correlate with HPLC analysis.

7. CONCLUSIONS AND FUTURE PERSPECTIVE

Enzyme sensors are reported here, and these sensors are simple, fast, sensitive, and used for the detection of various analytes. ENPs-based biosensors have exhibited good analytical performance in terms of detection limit and shelf life. In future, ENPs could be employed for designing biosensors, biomedical devices, biofuel cells, and enzyme-based reactors. These functionalized ENPs could be used as tags for bioaffinity assays of protein and DNA. Such biosensor technology may open new opportunities for biosensors, clinical diagnosis, and medical management.

CONFLICT OF INTEREST

All authors of this chapter have no conflict of interest.

REFERENCES

Aggarwal, V., Malik, J., Prashant, A., Jaiwal, P. K., & Pundir, C. S. (2016). Amperometric determination of serum total cholesterol with nanoparticles of cholesterol esterase and cholesterol oxidase. *Analytical Biochemistry*, *500*, 6–11.

Batra, B., Lata, S., Sharma, M., & Pundir, C. S. (2012). An acrylamide biosensor based on immobilization of haemoglobin onto multiwalled carbon nanotubes/copper nanoparticles/polyaniline hybrid film. *Analytical Biochemistry*, *433*, 210–217.

Blanchette, C., Lacayo, C. I., Fischer, N. O., Hawang, M., & Thelen, M. P. (2012). Enhanced cellulose degradation using cellulose nanospheres. *PLoS One*, *7*, 42–116.

Cammann, K. (1977). Biosensors based on ion-selective electrodes. *Fresenius Journal of Analytical Chemistry*, *287*, 1–9.

Cete, S., Yaşar, A., & Arslan, F. (2006). An amperometric biosensor for uric acid determination prepared from uricase immobilized in polypyrrole film. *Artificial Cells, Blood Substitutes, and Immobilization Biotechnology*, *34*(3), 367–380.

Chauhan, N., Kumar, A., & Pundir, C. S. (2014). Construction of an uricase nanoparticles modified Au electrode for amperometric determination of uric acid. *Applied Biochemistry and Biotechnology*, *174*, 1683–1694.

Chawla, S., Rawal, R., Sonia, R., & Pundir, C. S. (2013). Preparation of cholesterol oxidase nanoparticles and their application in amperometric determination of cholesterol. *Journal of Nanoparticle Research*, *15*, 1934–1943.

Chen, Y., Xiao, L., Liu, Y., Li, X., Zhanh, J., & Shu, Y. (2014). A lipase-based electrochemical biosensor for target DNA. *Microchimica Acta*, *181*, 615–621.

Coester, C. J., Langer, K., & Von, B. (2000). Gelatin nanoparticles by two step desolvation: A new preparation method, surface modification and cell uptake. *Journal of Microencapsulation*, (2), 187–193.

Dagar, K., & Pundir, C. S. (2017). An improved amperometric L-lactate biosensor based on covalent immobilization of microbial lactate oxidase onto carboxylated multiwalled carbon nanotubes/copper nanoparticles/polyaniline modified pencil graphite electrode. *Enzyme and Microbial Technology*, *96*, 177–186.

Deshapriya, I., Stromer, B. S., Kim, C. S., Patel, V., Gutkind, J. S., & Kumar, C. V. (2015). Novel, protein-based nanoparticles: Improved half-lives, retention of protein structure and activities. *Bioconjugate Chemistry*, *26*, 396–404.

Elif, B. B., & Mustafa, S. K. (2015). Applications of commercial biosensors in clinical, food, environmental and biothreat/biowarfare analyses. *Analytical Biochemistry*, *478*, 107–120.

Ezpeleta, I., Irchae, J. M., Stainmesses, S., Chabenat, C., Popineau, Y., & Orecchionic, A. M. (1999). Preparation of Ulex europaeus lectin-gliadin nanoparticle conjugates and their interaction with gastrointestinal mucus. *International Journal of Pharmaceutics*, *191*, 25–32.

Freitas, D. D. S., Spencer, P. J., Vasao, R. C., & Abrahao-Neto, J. (2009). Biochemical and biopharmaceutical properties of PEGylated uricase. *International Journal of Pharmaceutics*, *387*, 215–222.

Guo, M., Chen, J., Li, J., Nie, L., & Yao, S. (2004). Carbon nanotubes-based amperometric cholesterol biosensor fabricated through layer-by-layer technique. *Electroanalysis*, *16*, 1–4.

Kalia, V., Goyal, L., & Pundir, C. S. (1999). Determination of serum glucose with alkyl amine glass bound glucose oxidase. *Chinese Journal of Biotechnology*, *14*, 201–204.

Khosravi, A., Vossoughi, M., Sharokhian, S., & Alemzadeh, I. (2012). In *Synthesis and stability evaluation of HRP single enzyme nanoparticles. The proceedings of international conference on nanostructures (ICNS4)* (pp. 857–869).

Kim, J., & Grate, J. W. (2003). Single enzyme nanoparticles armored by a nanometer scale organic/inorganic network. *Nano Letters*, *3*, 1219–1222.

Kundu, N., Yadav, S., & Pundir, C. S. (2012). Preparation and characterization of glucose oxidase nanoparticles and their application in DO metric determination of serum glucose. *Journal of Nanoscience and Nanotechnology*, *13*, 1710–1716.

Liu, G., Lin, Y., Ostatna, V., & Wang, J. (2005). Enzyme nanoparticles based electronic biosensor. *Chemical Communications*, (27), 3481–3483.

Narwal, V., Yadav, N., Thakur, M., & Pundir, C. S. (2017). An amperometric H_2O_2 biosensor based on hemoglobin nanoparticles immobilized onto a gold electrode. *Bioscience Reports*, *37*, 1–10.

Nikalje, A. P. (2015). Nanotechnology and its applications in medicine. *Medicinal Chemistry*, *5*, 81–89.

Pundir, C. S. (2015). Introduction to enzyme and nanotechnology. In A. Cooper (Ed.), *Enzyme nanoparticles: Preparation, characterization, properties, and applications (micro and nanotechnology series)*. Oxford, UK: Elsevier.

Pundir, C. S., & Aggarwal, V. (2017). Amperometric triglyceride bionanosensor based on nanoparticles of lipase, glycerol kinase, glycerol-3-phosphate oxidase. *Analytical Biochemistry*, *517*, 56–63.

Roco, M. C. (2003). Converging science and technology at the nanoscale: Opportunities for education and training. *Nature Biotechnology*, *21*, 1247–1249.

Sailaja, A. K., Amareshwar, P., & Chakravarty, P. (2011). Different techniques used for the preparation of nanoparticles using natural polymers and their application. *International Journal of Pharmacy and Pharmaceutical Sciences*, *3*, 45–50.

Scheffel, U., Rhodes, B. A., Natrajan, T. K., & Wagner, H. N. (1972). Albumin microspheres for study of reticuloendothelial system. *Journal of Nuclear Medicine*, *13*, 498–503.

Sharma, S., Shrivastav, A., Gupta, N., & Srivastava, S. (2011). In *Amperometric biosensor: Increased sensitivity using enzyme nanoparticles. 2010 international conference on nanotechnology and biosensors, IPCBEE (Vol. 2)* (pp. 24–26).

Shukla, S. K., Deshpande, S. R., Shukla, S. K., & Tiwari, A. (2012). Fabrication of a tunable glucose biosensor based on zinc oxide/chitosan-graft-poly(vinylalcohol) core-shell nanocomposite. *Talanta*, *99*, 283–287.

Shukla, S. K., Mishra, A. K., Mamba, B. B., & Omotayo, A. A. (2014). Zirconia-poly (propylene imine) dendrimer nanocomposite based electrochemical urea biosensor. *Enzyme and Microbial Technology*, *66*, 48–55.

Silva, G. A. (2004). Introduction to nanotechnology and its applications to medicine. *World Neurosurgery*, *61*, 216–220.

Stromer, B. S., & Kumar, C. V. (2016). White-emitting protein nanoparticles for cell-entry and pH sensing. *Advanced Functional Materials*, *27*, 1603874–1603879.

Turner, A., Karube, I., & Wilson, G. S. (Eds.), (1987). *Biosensors: Fundamentals and applications*. Oxford, UK: Oxford University Press p. V.

Valipour, M. (2015). *Handbook of environmental engineering problems*. Foster City, CA: OMICS Group eBook, pp. 1–77.

Varma, R., & Nene, S. (2003). Biosynthesis of cholesterol oxidase by Streptomyces lavendulae NCIM 2421. *Enzyme and Microbial Technology*, *33*, 286–291.

Wang, X., Piro, B., Reisberg, S., Anquetin, G., Rocquigny, H. D., Jiang, P., et al. (2014). Direct, reagentless electrochemical detection of the BIR3 domain of X-linked inhibitor of apoptosis protein using a peptide-based conducting polymer sensor. *Biosensors & Bioelectronics*, *61*, 57–62.

Yadav, N., Chhillar, A. K., & Pundir, C. S. (2018). Preparation, characterization and application of haemoglobin nanoparticles for detection of acrylamide in processed foods. *International Journal of Biological Macromolecules*, *107*, 1000–1013.

FURTHER READING

Bahadir, E. B., & Mustafa, S. K. (2015). Applications of commercial biosensors in clinical, food, environmental and biothreat/biowarfare analyses. *Analytical Biochemistry*, *478*, 107–120.

Choudhary, M., Shukla, S. K., Taher, A., Siwal, S., & Kaushik, M. (2014). Organic–inorganic hybrid supramolecular assembly: An efficient platform for nonenzymatic glucose sensor. *ACS Sustainable Chemistry & Engineering*, *2*, 2852–2858.